R.R. Haese, T. LaForce, C. Boreham, J. Ennis-King, B.M. Freifeld, L. Paterson, U. Schacht

Determining residual CO_2 saturation through a dissolution test – Results from the CO2CRC Otway Project

11th International Conference on Greenhouse Gas Control Technologies (GHGT-11); Energy Procedia, vol. 37, 2013 / vol.37, pp.5379-5386

Originally published at:
http://doi.org/10.1016/j.egypro.2013.06.456

Available online at www.sciencedirect.com

SciVerse ScienceDirect

Energy Procedia 37 (2013) 5379 – 5386

Energy Procedia

GHGT-11

Determining residual CO_2 saturation through a dissolution test – Results from the CO2CRC Otway Project

R.R. Haese[a]*, T. LaForce[b], C. Boreham[a], J. Ennis-King[b], B.M. Freifeld[c], L. Paterson[b], U. Schacht[d]

[a]*CO2CRC, Geoscience Australia, GPO Box 378, Canberra ACT 2601, Australia*
[b]*CO2CRC, CSIRO Earth Science and Resource Engineering, Private Bag 10, Clayton South, Victoria 3169, Australia*
[c]*Lawrence Berkeley National Laboratory, MS 90-1116, One Cyclotron Road, Berkeley, CA 94720, USA*
[d]*CO2CRC, Australian School of Petroleum, University of Adelaide, South Australia 5005, Australia*

Abstract

Residual CO_2 trapping (Sgr-CO_2) is a key mechanism for geological CO_2 storage. The CO2CRC undertook a sequence of field tests with the aim of comparing different ways of determining Sgr-CO_2 including a dissolution test. Dissolution test results show an unexpectedly early breakthrough and low maximum CO_2 concentrations in the back-produced water making the data inconclusive when using traditional data interpretation. Here, we consider two conditions to explain the observations: Firstly, residual CO_2 is vertically unevenly distributed and, secondly, the fluid and residual CO_2 are not in equilibrium. Furthermore, we postulate localised flow channels have formed during the 3-month test period caused by advective flow of CO_2-saturated, low pH water leading to transport-controlled mineral dissolution.

Selection and/or peer-review under responsibility of GHGT

Keywords: storage capacity; single well test; residual CO2; heterogeneity

1. Introduction

Capture and geological storage of CO_2 from major industrial sources is seen as one important measure to mitigate the global increase in atmospheric CO_2 and associated climate change. For the purpose of geological storage site selection and the assessment of short- to long-term storage security, it is important to quantify the trapping mechanisms for CO_2 in the storage reservoir. Four principal trapping mechanisms

* Corresponding author. Tel.: +61-3-90353055; *E-mail address:* ralf.haese@unimelb.edu.au.

1876-6102
Selection and/or peer-review under responsibility of GHGT
doi:10.1016/j.egypro.2013.06.456

have been identified [1]: structural trapping, residual trapping, dissolution trapping and mineral trapping. Residual trapping is the immobilisation of supercritical CO_2 by capillary forces or by the enclosure in pores preventing further CO_2 migration by buoyancy or in response to a pressure gradient. Residual trapping is considered one of the key trapping mechanisms for geological CO_2 storage and is of particular importance in formations without proven structural closure. It is quantified by determining the residual gas saturation (Sgr-CO_2), which has been achieved on cores in laboratory experiments [2], but not at field scale using single well tests. This circumstance introduces uncertainty in the prediction of the nature and capacity of CO_2 storage and would benefit from the development of single-well test procedures.

The Cooperative Research Centre for Greenhouse Gas Technologies (CO2CRC) commissioned the drilling and completion of a dedicated well (CRC-2) with perforations in the Paaratte Formation of the Otway Basin, Australia, with the aim to develop and compare six methods to determine Sgr-CO_2 in the field. The rationale for the design of the field experiment is given by Zhang et al. [3] and an overview of the experiment's execution is provided by Paterson et al. [4]. The dissolution test is one of these six methods applied during a test sequence, which was carried out from June to September 2011.

2. Reservoir conditions

The target reservoir is located within the Paaratte Formation, which is an interbedded sandstone and mudstone sequence deposited in multiple progradations of delta lobes during the Campanian. The CRC-2 well is located at the CO2CRC demonstration site near Port Campbell, Victoria, and the well perforation is within the Paaratte Formation at a depth between 1392 and 1399 m TVDSS (true vertical depth below sea level). The *in situ* temperature is 59°C and the hydrostatic pressure is 14.2 MPa. The average permeability is 2.1 darcies and the average porosity is 28% [4]. The total dissolved solid concentration (TDS) of the formation water is very low at approximately 900 mg/L during initial water production. The lithology of the perforated interval is a quartz-dominated sandstone with 44 wt% quartz, moderate amounts of kaolinite and mica (each 11 wt%), and minor amounts of chlorite (6 wt%), K-feldspar (5 wt%), pyrite and rutile (3 wt% each) and 18 wt% of unidentified amorphous phase. Above and below the perforated interval, the sediment is highly cemented by carbonate minerals (25 – 28 wt% dolomite, 7 – 8 wt% ankerite).

3. Methods

3.1. Field test conditions

The dissolution test was carried out at the end of a 3-month test sequence comparing six methods for the determination of Sgr-CO_2. Starting on 17 June 2011, 510 tonnes of water was initially produced and stored at the surface (Phase 1), for use in later water injections. Several baseline characterisation tests were conducted following the initial water production (Phase 2). Residual CO_2 gas was formed by injecting 150 tonnes of CO_2 at a rate of 37.5 tonnes per day followed by the concurrent injection of 454 tonnes of water and 26.2 tonnes of CO_2 over three days. Water and CO_2 were mixed in the well using a gas mandrel at a depth of 798 m TVDSS (Phase 3). A series of characterisation tests in the presence of residual CO_2 were carried out including the injection and back-production of the noble gas tracers krypton and xenon dissolved in CO_2 saturated water (Phase 4). Finally, the dissolution test was carried out by injecting 75 tonnes of water over half a day, immediately followed by the back-production of 119 tonnes over 2.5 days (Phase 5). Details of the residual gas saturation test sequence are given by Paterson et al. [4].

The procedure of the applied dissolution test is based on the Bragg et al. method [5], which was developed to determine residual methane saturation. As the injection water has a very low CO_2 concentration (0.01 mol/L) it dissolves residual CO_2 progressively outward from the well during injection. The dissolved CO_2 concentration in the injected water rises in the reservoir to its maximum concentration equivalent to the CO_2 saturation concentration (1.05 mol/L) under the given pressure, temperature and total dissolved solid concentration conditions (Fig. 1).

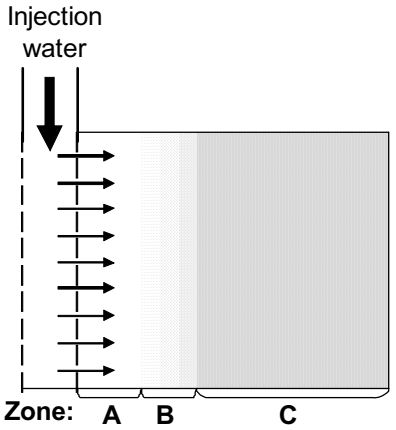

Figure 1: Conceptual representation of the dissolution test. Three zones can be distinguished: Zone A refers to the zone of water with no CO_2, Zone B is the active dissolution zone and Zone C is the remaining reservoir with residual CO_2 and CO_2 saturated water.

3.2. Sampling and analytical methods

Formation water and its dissolved gas were sampled using the U-tube system, which allows collection of a) a fluid sample under reservoir pressure and b) a gas sample derived from the exsolved gas at reduced pressure (6.2 MPa). U-tube samples were taken continuously approximately every 1.5 hours during the 62.5 hours of water production period leading to the collection of 40 samples.

Fluid samples were collected in two 150 ml stainless steel cylinders at reservoir pressure. One sample cylinder was used for the analysis of the dissolved inorganic carbon (DIC, DIC = ΣCO_2, HCO_3^-, CO_3^{2-}) concentration. The other sample cylinder was used for analysis of general water properties (temperature, pH, total dissolved solid concentration, alkalinity) analysed on site and subsamples were taken for further analysis at Geoscience Australia's laboratories. NaOH was mixed with the formation water for DIC analysis in a closed system to avoid CO_2 escape from the fluid during depressurisation. DIC was analysed on site using an AS-C3 model DIC analyser by Apollo SciTech, which includes an infrared-based CO_2 detector (LiCor 7000).

Methanol was added at a concentration of ~0.1wt% during the injection phase of the dissolution test to act as a conservative tracer. Methanol was analysed by gas chromatography with on-column injection, helium as a carrier gas and a methanizer-flame ionization detector.

Gas samples were collected in Isotubes® and gas bags and analysed on site. The molecular composition of CO_2, N_2, O_2 and $C_1 - C_5$ wet gas components were analysed on an SRI Multiple Gas Analyzer using helium as carrier gas. CO_2 is detected by the FID after being converted to CH_4 in the methanizer. A second SRI Multiple Gas Analyzer with helium as carrier gas, a customised column configuration and a pulsed discharge- helium ionisation detector was used for Kr and Xe detection. In situ

dissolved CO_2 concentrations were calculated from CO_2 concentrations in exsolved gas samples using a calibration derived at the test site. Further details of the gas analysis can be found in Boreham et al. [6].

3.3. Modelling

The two-dimensional distribution of Sgr-CO_2 for a full-field model before and after the dissolution test was modelled in TOUGH2 using the downhole pressure data and the surface measurements for the rates of injection and production of water and CO_2 (Figure 2).

To study the details of the dissolution test in isolation from the rest of the residual tests, simple radial models were constructed for dissolution. Forward modeling included the injection and back-production of water with the non-reactive methanol tracer. Fluid injection and production rates were the average rate obtained in the field, and the length of injection was also based on field data [4].

Initially, the seven meter perforated reservoir interval was treated as one homogenous layer with 21% residual gas saturation and equilibrium between the fluid and residual CO_2 was assumed. (Figure 5 a and b). The computer code TOUGH2 [7] was used for simulations of the homogenous reservoir with equilibrium between fluid and residual CO_2.

Secondly, the targeted reservoir interval was split into three horizontal layers. The top and bottom layers have a residual gas saturation of 21%, whereas the intermediate layer has no residual gas saturation. The code UTCHEM [8] was validated against the TOUGH2 equilibrium results before it was used for the multilayer, non-equilibrium simulations. Disequilibrium is modeled in UTCHEM using the Sherwood number. The following fitting parameters were chosen: $ß_0 = 10$, $ß_1 = 0.33$, $ß_2 = 0.67$, $ß_3 = 0.42$, based on packed spherical bead experiments on groundwater contaminants [9]. A vertical to horizontal permeability ratio of 1:10 was used. In the UTCHEM results gravity had no discernible influence on the results; therefore, the layering impacted only the overall maximum CO_2 production, but not the shape of the breakthrough curve.

4. Results

The radial simulation of the Sgr-CO_2 distribution at the beginning and the end of the dissolution test is shown in Figure 2. The Sgr-CO_2 plume has its maximum extent at the top of the reservoir driven by the buoyancy of supercritical CO_2. At the beginning of the dissolution test a maximum of 26% Sgr-CO_2 is reached in the top metre of the reservoir extending approximately 2 metres outward from the well. Only 2 metres below, Sgr-CO_2 drops to 16%. After the dissolution test, a 2-metre zone devoid in residual CO_2 has developed adjacent to the well reflecting the effective dissolution of CO_2 during the test. In the top metre of the reservoir, however, the CO_2-devoid zone is less than 50 centimetres.

The rise in dissolved inorganic carbon (DIC) concentration in fluid and exsolved gas samples occurs approximately between 7.5 and 25 tonnes of produced water. After 25 tonnes, the two independently measured concentrations reach a plateau with their maximum concentrations (Fig. 3a). The maximum DIC concentration derived from fluid samples varies approximately between 0.3 and 0.4 mol/L, and the maximum DIC concentration derived from exsolved gas samples is consistently close to 0.7 mol/L. These concentrations are significantly below the expected CO_2 saturation concentration of 1.05 mol/L. The noble gas concentrations krypton (Kr) and xenon (Xe) in exsolved gas samples rise simultaneously with DIC reaching their maximum concentrations at 20 tonnes of produced water before they decline exponentially (Fig. 3b).

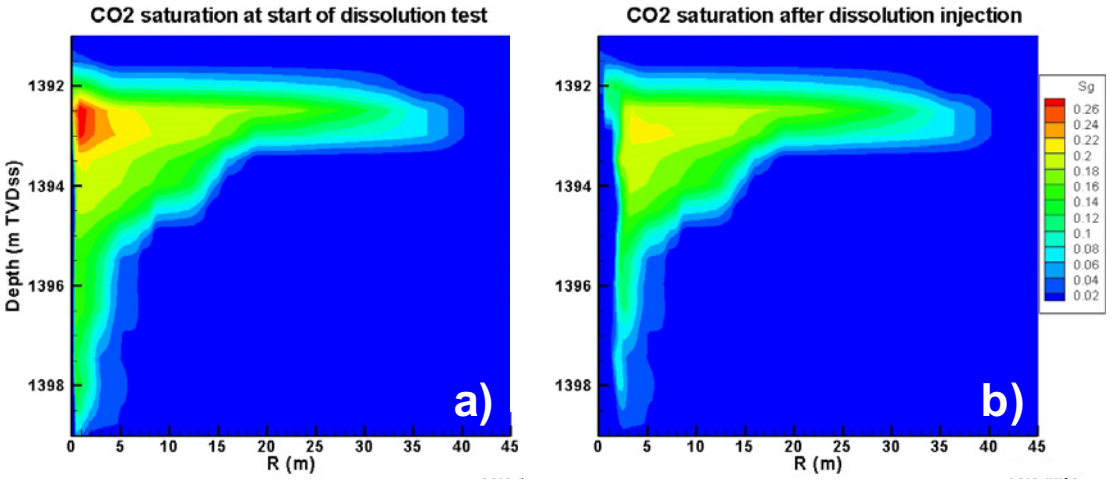

Figure 2: Modelled two dimensional distribution of residual gas saturation before (a) and after (b) the dissolution test. R is the radius from the well outward. Note, the CO_2-devoid zone adjacent to the well after the dissolution test (b) shows the effective dissolution of CO_2 during the test.

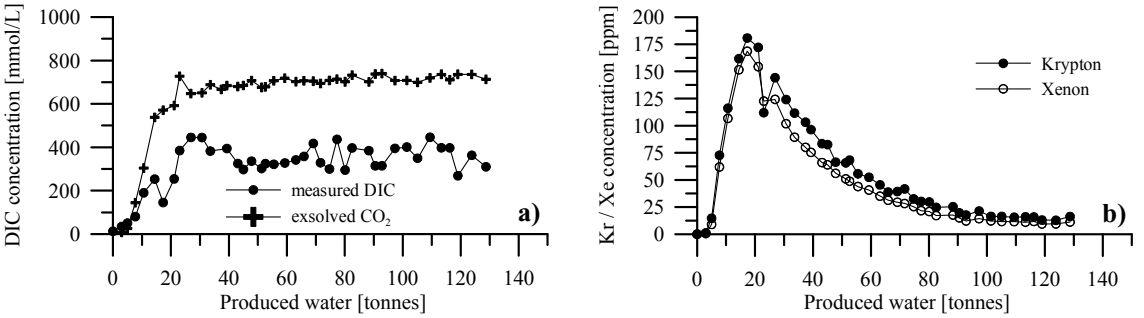

Figure 3: (a) Dissolved inorganic carbon (DIC) concentrations measured in fluid samples and calculated from exsolved gas concentrations and (b) krypton (Kr) and xenon (Xe) concentrations in exsolved gas samples. [ppm] refers to a volumetric gas concentration.

The concentration of the non-reactive tracer methanol stays at the injection concentration of 1200 mg/L from 0 to 35 tonnes of produced water before gradually declining towards zero (Fig. 4a). The average total dissolved solid (TDS) concentration during the initial water production of the test sequence was 906 mg/L (Phase 1), 1011 mg/L during the baseline characterisation test (Phase 2), 1161 mg/L during the residual CO_2 characterisation test (Phase 4) and 1324 mg/L during the dissolution test at the end of the experiment (Phase 5) (Fig. 4b).

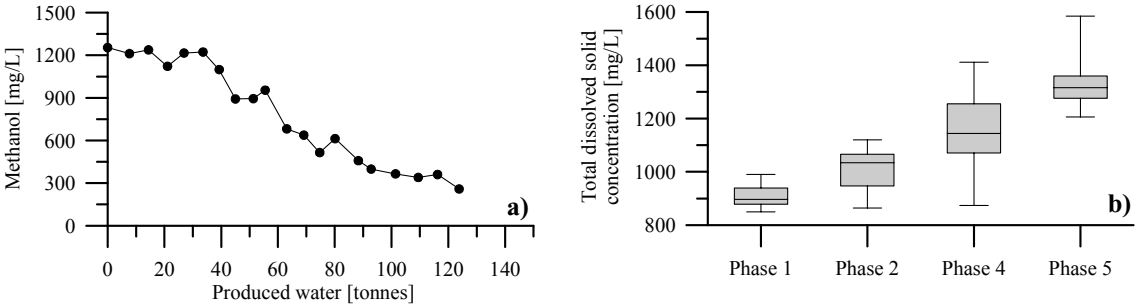

Figure 4: (a) Methanol concentrations during the dissolution test and (b) total dissolved solid concentrations (TDS) during different test phases. Horizontal bars represent means, upper and lower boundaries of boxes represent upper and lower quartiles, respectively, and upper and lower caps represent maximum and minimum values, respectively.

The simplified radial model simulations show a significant dependence of the CO_2 breakthrough on Sgr-CO_2 with the earliest breakthrough at high (e.g. 40%) and late breakthrough at low (e.g. 5%) Sgr-CO_2 values (Fig. 5a). In contrast, the methanol tracer concentration declines between 40 and 80 tonnes of produced water with little dependency on the residual gas saturation, as expected (Fig. 5b). The difference in CO_2 and methanol behaviour results from the accumulation of CO_2 as a function of residual gas concentration forming a plume front preceding the plume tail of methanol.

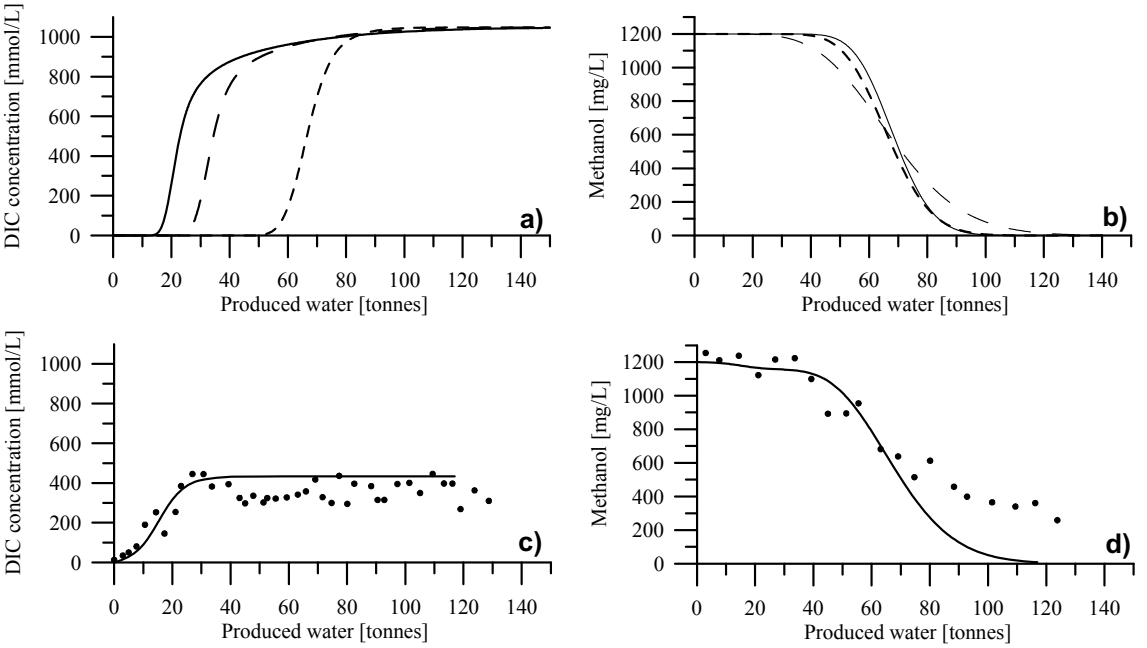

Figure 5: Modelling results for dissolved inorganic carbon and methanol concentrations assuming fluid – residual CO_2 equilibrium in a single-layer, homogenous reservoir (a and b) and assuming disequilibrium in a three-layer reservoir (c and d). In panels a and b, the short-stippled line, the long-stippled line and the full line represent 5, 20 and 40% residual CO_2. In panel c and d, dots represent measured data.

5. Discussion

An early and concurrent breakthrough of CO_2 in the back-produced water resulting from the dissolution of residual CO_2 is observed in the measurements of DIC in fluid samples and derived from exsolved gas samples. The early CO_2 breakthrough is further confirmed by the concurrent rise in Kr and Xe concentrations, which must be mobilised from residual CO_2 enriched in these noble gases during a previous experiment sequence (Phase 4). Based on 1D single layer simulations, such an early breakthrough in CO_2 suggests a residual CO_2 abundance of approximately 40%. This estimate is, however, unrealistic when compared to the pulsed neutron reservoir saturation tool (RST) logs and radial simulations based on pressure data with Sgr-CO_2 values in the range of 23 to 18 and 26 to 10%, respectively. It is further noted the maximum DIC concentrations as measured in fluid samples and derived from exsolved gas samples are distinctively below the expected saturation concentration of 1.05 mol/L. Some CO_2 loss from fluid samples could have been caused by degassing during the opening of the stainless steel cylinders, yet, this artifact was attempted to be prevented by the addition of NaOH. The integrity of DIC concentrations derived from exsolved gas samples appears good given the consistent trend and little scatter in the data.

The observed decline in methanol concentration over time is more gradual in the experimental data compared to simulation results. This gradual decline suggests a larger effective dispersion than expected, which may result from averaging across a heterogeneous vertical section in 1D simulation [10].

The above observations and the full-project simulation results (Fig. 2) suggest a vertically variable distribution of residual CO_2 and guided fluid flow simulations in a heterogeneous reservoir. Simulations of water injection into and back-production from the simplified multi-layer reservoir with variable residual CO_2 concentrations provide an explanation for maximum observed CO_2 concentrations below saturation, however, layering does not impact the breakthrough time of the CO_2 in the simulations. A model considering disequilibrium between residual CO_2 and water at the reservoir simulation scale results in a slow dissolution rate and more gradual rise in the CO_2 concentration (Fig. 5c). Such a disequilibrium could be, for example, caused by a small surface area to volume ratio of residual CO_2. As an analogy, the volume of residual oil clusters can vary over four orders of magnitude with a maximum volume above 1 mm^3 [11]. However, given the lack of experimental data on CO_2 dissolution rates in heterogeneous porous media, we do not know how likely it is that this mechanism impacted the field test. Despite the various model assumptions, the long asymptotic decrease in the methanol profile cannot be reproduced.

In addition to vertically variable residual CO_2 abundance, an increase in vertical reservoir heterogeneity may be caused by the imposed fluid advection during injection and back-production of CO_2-saturated water with a low pH. Reactive infiltration instability occurs when a fluid passes through a porous media with permeability heterogeneity at pore scale resulting in the formation of localised flow channels with high, transport-controlled mineral dissolution rates [12]. The flow channels, also referred to fingers or wormholes, propagate into the host rock more rapidly than a reactive front in a homogeneous media and are characterised by increased porosity and permeability due to mineral dissolution. Slower, surface-controlled dissolution rates are expected in periods between well operations. Net mineral dissolution throughout the test sequence is evident from the total dissolved solid concentration increase from an average of 900 to above 1300 mg/L. Based on preliminary water composition data and aqueous speciation modelling, CO_2 saturation leads to a drop in pH from 7.7 to 4.2 and to significant undersaturation in chlorite, K-feldspar, calcite and dolomite (data not shown) contained in the reservoir rock. In addition, pyrite could have dissolved due to the exposure to oxic injection water.

6. Conclusions

While more detailed studies on mineral dissolution are outstanding, the presented data and theoretical considerations suggest an increase in reservoir heterogeneity caused mineral dissolution during the test sequence under CO_2 saturated conditions. Heterogeneity in the distribution of residual CO_2 and a potential disequilibrium between fluid and residual CO_2 at the reservoir scale currently do not allow for a consistent determination of *in situ* Sgr-CO_2 using the dissolution test data.

Acknowledgements

The authors wish to thank Rajindar Singh from the CO2CRC, Linda Stalker from CSIRO, Jay Black, Teagan Exposito, Janice Trafford and Eleena Wykes from Geoscience Australia, and the personnel from AGR for their support at the Otway site during the test. Eric Tenthorey and Jay Black provided valuable comments on an earlier version of the manuscript. Funding was provided by the Australian Government through its CRC Program to support this research. The authors acknowledge financial assistance provided through Australian National Low Emissions Coal Research and Development (ANLEC R&D). ANLEC R&D is supported by Australian Coal Association Low Emissions Technology Limited and the Australian Government through the Clean Energy Initiative. This publication has received permission for publication by the CEO of Geoscience Australia.

References

[1] Intergovernmental Panel on Climate Change. Special Report on CO_2 Capture and Storage, edited; 2005: 208-210.

[2] Saeedi A, Rezaee R, Evans B, Clennell B. Multiphase flow behaviour during CO_2 geo-sequestration: Emphasis on the effect of cyclic CO_2-brine flooding. *J Petr Sci Eng* 2011;**79**:65-85.

[3] Zhang Y, Freifeld BM, Finsterle S, Leahy M, Ennis-King J, Paterson L, Dance T. Single-well experimental design for studying residual trapping of supercritical carbon dioxide. *IJGGC* 2011;**5**:88-98.

[4] Paterson L, Boreham C, Bunch M, Dance T, Ennis-King J, Freifeld BM, Haese RR, Jenkins C, LaForce T, Raab M, Singh R, Stalker L, Zhang Y. Overview of the CO2CRC Otway residual saturation and dissolution test. *Energy Procedia* this issue 2012.

[5] Bragg JR, Shallenberger LK, Deans HA. In-situ determination of residual gas saturation by injection and production of brine. SPE 6047, 51st Annual Fall Technical Conference of the Society of Petroleum Engineers, New Oleans, USA, Oct 3-6 1976.

[6] Boreham C, Underschultz J, Stalker L, Kirste D, Freifeld B, Jenkins C, Ennis-King J,. Monitoring of CO_2 storage in a depleted natural gas reservoir: Gas geochemistry from the CO2CRC Otway Project, Australia. *IJGGC* 2011;**5**:1039–1054.

[7] Pruess K, Oldenburg C, Moridis G. TOUGH2 user's guide, version 2.0. Lawrence Berkeley National Laboratory, Berkeley, USA, 1st edition, 1999.

[8] Reservoir Engineering Research Program. Volume II: Technical documentation for UTCHEM-9.0: A three-dimensional chemical flood simulator. University of Texas, Austin, USA, 1st edition, 2000.

[9] Powers SE, Loureiro CO, Abriola LM, Weber Jr WJ. Theoretical study of the significance of non-equilibrium dissolution of nonaqueous phase liquids in subsurface systems. *Water Res Res* 1991;**27**: 463-477.

[10] Arya A, Hewett TA, Larson RG, Lake LW. Dispersion and reservoir heterogeneity. *SPE Res Eng* 1988; **3**:139-148.

[11] Karyn ZT, Piri M, Singh G. Experimental investigation of trapped oil clusters in a water-wet bead pack using X-ray microtomography. *Water Res Res* 2010;**46**, doi:10.1029/2008WR007539.

[12] Ortoleva P, Chadam J, Merino E, Sen A. Geochemical self-organisation II: The reactive-infiltration instability. *Am J Sci* 1987;**287**:1008-1040.